



LAWRENCE
LIVERMORE
NATIONAL
LABORATORY

Radiation multigroup diffusion for refractive, lossy media in ALE3D (U)

A. I. Shestakov

December 20, 2010

NECDC

Los Alamos, NM, United States

October 18, 2010 through October 22, 2010

This document was prepared as an account of work sponsored by an agency of the United States government. Neither the United States government nor Lawrence Livermore National Security, LLC, nor any of their employees makes any warranty, expressed or implied, or assumes any legal liability or responsibility for the accuracy, completeness, or usefulness of any information, apparatus, product, or process disclosed, or represents that its use would not infringe privately owned rights. Reference herein to any specific commercial product, process, or service by trade name, trademark, manufacturer, or otherwise does not necessarily constitute or imply its endorsement, recommendation, or favoring by the United States government or Lawrence Livermore National Security, LLC. The views and opinions of authors expressed herein do not necessarily state or reflect those of the United States government or Lawrence Livermore National Security, LLC, and shall not be used for advertising or product endorsement purposes.

This work performed under the auspices of the U.S. Department of Energy by Lawrence Livermore National Laboratory under Contract DE-AC52-07NA27344.

Radiation multigroup diffusion for refractive, lossy media in ALE3D (U)

A. I. Shestakov and J. S. Stölken

Lawrence Livermore National Laboratory
Livermore CA

We describe development of radiation multigroup diffusion module RADMGDIFF in LLNL's code ALE3D. RADMGDIFF was initially developed to model radiation flow in a homogeneous, refractive, absorptive medium, specifically, silica (SiO_2). The intended application modeled a proposed procedure for surface damage mitigation of final NIF optics. For such experiments, one models rapid heating and cooling of a silica disk. Heating stems from energy deposited by a laser whose energy is deposited effectively on the surface thereby raising the local temperature. Heat propagates into the material via conduction and radiation transport. Heat escapes by means of radiation, and to a lesser extent, by convection. Derivation of the appropriate radiation diffusion equations appear in Shestakov *et al* [11]. Here, we summarize the Shestakov *et al* paper and describe recent, related work and enhancements to RADMGDIFF. Most notably, we define a different fundamental variable ξ , the integral over direction of the intensity divided by the square of the refractive index. Using ξ leads to a succinct expression for a condition at an internal material interface. The interface condition is a generalization of the boundary condition derived in Shestakov *et al* [11] for a planar air-silica interface that incorporates reflectivities obtained from the Fresnel relations. RADMGDIFF may also be used for conventional multigroup diffusion calculations, i.e., for materials with refractive indexes equal to one. We compare results with Lasnex on a problem that models cooling of two adjacent hot slabs in which the opacity varies with temperature. We present results on a 3D version of the "Crooked Pipe" aka "Tophat" test problem of Graziani [4] and Gentile [5]. (UNC)

Prepared for Proceedings of the NECD 2010 _____

UNCLASSIFIED

Introduction

Radiation is often ignored in relatively low temperature regimes ($T < 8000$ °K) due to its low energy content. Nevertheless, radiation is still an efficient vehicle for energy (heat) transport and loss. Its importance as an effective heat transfer mechanism for glass has long been recognized. Gardon [3] and Condon [2] present valuable surveys of the process. Early work modeled the enhanced energy transfer due to radiation by adding to the conventional energy flux $k_m \nabla T$ a gray radiative heat flux proportional to $n^2 \sigma T^4$, where n is the medium's (in this case, frequency averaged) refractive index and σ is the Stefan-Boltzmann constant. In this model, the radiation field is assumed to be tightly coupled to the medium. Hence, the radiation spectrum equals the matter emission source $n^2 \mathcal{B}_\nu(T)$, where $\mathcal{B}_\nu(T)$ is the Planck function. Tight coupling requires a large opacity for *all* frequencies. However, for glass in general and silica (SiO_2) in particular, the absorptivity has a complicated spectral structure, as displayed in Figure 1. At room temperature, in the IR-visible part of the spectrum ($\lambda \approx 1 \mu\text{m}$, $\nu \approx 1 \text{ eV}$) the medium is transparent; the opacity $\kappa \approx 0.01 \text{ cm}^{-1}$. However, it is quite opaque for certain smaller photon energies; at $\nu \approx 0.13 \text{ eV}$ $\kappa > 10^4$, an increase of 10^6 . Thus, we do not have tight coupling for all ν , which implies one should evolve a separate equation for the radiation field. In principle, the equation could evolve the average of radiation intensity over direction of propagation and frequency; effectively, an equation for a radiation temperature T_r . However, modeling radiation with only a T_r equation can yield erroneous results. The T_r equation is the limiting case (a single group) of a multigroup formulation. A multigroup equation stems from discretizing the frequency variable into a finite number of groups. Results in Shestakov *et al* [11] show that the quality of the result degrades as the frequency discretization is coarsened, thereby demonstrating the need for a multigroup system.

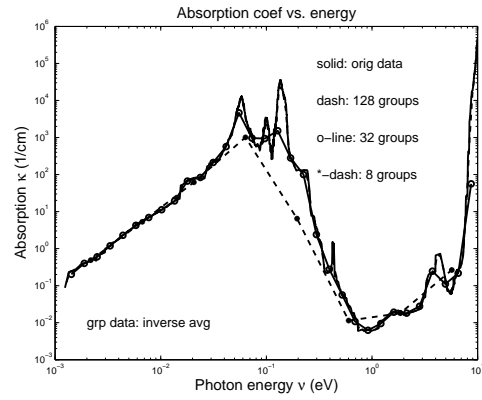


Figure 1: Opacity κ (cm^{-1}) vs. photon energy ν (eV) and three group averaged analogues. Data digitized from Kitamura *et al* [8].

Derivation of equations

In the following, unless noted otherwise, we use CGS units. Ignoring material motion, two equations model the relevant physics. The first governs material internal energy flow, i.e., heat conduction,

$$C \partial_t T = \nabla \cdot k_m \nabla T + S - K_{r,m}. \quad (1)$$

In Eq.(1), C is the heat capacity, k_m the conductivity, S an external energy source (e.g., a laser) and $K_{r,m}$ is the rate of energy exchange between radiation and the medium; it's sign depends on whether locally the radiation is "hotter" than the matter.

The second equation describes radiation energy transport and energy exchange with the medium. For homogeneous¹, refractive lossy media, we begin with the equation derived by Pomraning [10] to which we add coupling due to absorption,

$$(1/v_g) \partial_t (I/n^2) + \mathbf{\Omega} \cdot \nabla (I/n^2) = (\kappa/n^2) [n^2 \mathcal{B}_\nu(T) - I]. \quad (2)$$

¹In a homogeneous medium, the index of refraction, opacity, and hence, group speed are independent of space and time.

The LS of Eq.(2) differs from Pomraning's [10] Eq.(5.64) et seq. since we ignore spatial and temporal changes of n .

In Eq.(2), the intensity I depends on time, position, propagation direction Ω , and frequency ν . The equation introduces the group speed v_g , the opacity κ and the Planck function,

$$\mathcal{B}_\nu(T) = \frac{2h\nu^3/c^2}{\exp(h\nu/kT) - 1},$$

where h and k are the Planck and Boltzmann constants, resp., and c is the vacuum light speed. Note that in refractive media, radiation emission is given by $n^2 \mathcal{B}_\nu$ and radiation propagates at the frequency-dependent group speed v_g , which is related to the phase speed v_p , Born & Wolf [1],

$$v_g = v_p \left/ \left(1 + \frac{\nu}{n} \frac{dn}{d\nu} \right) \right., \quad v_p = c/n.$$

By taking moments of Eq.(2), Shestakov *et al* [11] derive two equations containing the spectral energy density,

$$E = (1/v_g) \int_{4\pi} d\omega I, \quad (3)$$

the flux, and the pressure tensor. A single equation is obtained by ignoring the temporal derivative of the flux and expressing the tensor, in the usual way, by a third of the energy density. The result is the multifrequency diffusion equation,

$$\partial_t E - \nabla \cdot \frac{v_g}{3\kappa} \nabla E = \kappa [4\pi n^2 \mathcal{B}_\nu(T) - v_g E]. \quad (4)$$

The coupling term $K_{r,m}$ introduced in Eq.(1) is the integral of the RS of Eq.(4) over all frequencies.

The RS of Eq.(4) has an interesting implication for multiple materials. Consider abutting media with distinct indexes n and group speeds. Approximate the v_g 's by the respective phase speeds c/n . Assume the materials are at a common temperature T . Equation (4) holds inside each material. If the

radiation field is in LTE, the RS of Eq.(4) is zero. Thus, in LTE the spectral radiation energies necessarily differ by the ratio $(n_a/n_b)^3$, where $n_{a,b}$ are the material indexes. However, distinct energies means E is discontinuous across the interface. The discontinuity could be resolved by diffusion, i.e., radiation (heat) flow across the interface. The flowing radiation couples to the media thereby leading to a temperature change, i.e., T would no longer be constant; clearly, an impossibility. The conundrum is discussed in the section where we derive interface conditions.

Boundary, interface conditions

In transport, radiation energy propagates along direction (rays) Ω . At an interface of two materials, incoming radiation is reflected and, depending on material properties and the incoming ray's angle of incidence, radiation can also be transmitted across the interface. Figure 2 displays a typical boundary or internal interface between materials a and b . Symbols $\Omega_{a,i}$ and $\Omega_{b,i}$ denote incoming rays from materials a and b , resp. Symbols $\Omega_{a,r}$ and $\Omega_{b,r}$ denote reflected rays. Symbol $\Omega_{a,t}$ denotes the transmitted ray. In the figure, there is no transmitted ray $\Omega_{b,t}$; all energy carried by $\Omega_{b,i}$ is specularly reflected. The fraction of energy in the incoming ray Ω_i carried away by the reflected ray Ω_r is determined by the reflectivity $R(\mu)$, where $\cos \mu = \Omega_i \cdot \hat{n}$ and \hat{n} is the interface normal.

Boundary condition

Here, we summarize the derivation in [11]; it is based on work of Larsen *et al*, [9]. Assume Fig.2 represents part of the boundary. Equations are solved in material b . In material a , the radiation field is assumed to be *diffusive*; it is specified by the Planckian field $\mathcal{B}_\nu(T_a)$, where T_a is known.

For transport, intensity emanating from the boundary $I_b(\Omega)$ must be specified. In a refractive medium, it consists of two parts,

$$I_b(\Omega) = I_{b,t}(\Omega) + I_{b,r}(\Omega). \quad (5)$$

Prepared for Proceedings of the NECD 2010

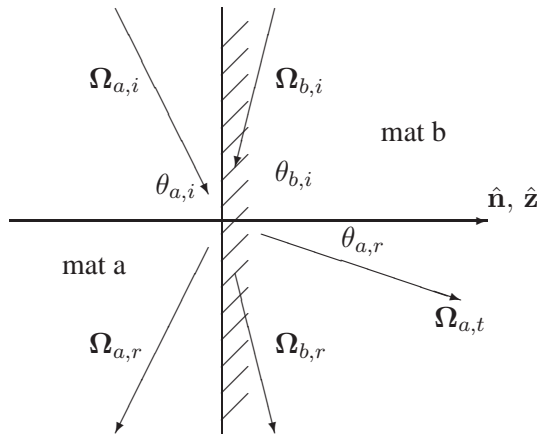


Figure 2: Schematic of rays across boundary or material interface.

In Eq.(5), $I_{b,t}$ represents intensity transmitted from the exterior, i.e., due to $\mathcal{B}_\nu(T_a)$. Analogously, $I_{b,r}$ represents the fraction of intensity directed toward the boundary that is reflected. Both $I_{b,t}$ and $I_{b,r}$ depend on the reflectivity $R(\mu)$. For diffusion, Eq.(5) is satisfied by integrating over the hemisphere inside b . The integration requires computing moments of $R(\mu)$,

$$r_j \doteq \int_0^1 d\mu \mu^j R(\mu), \quad j = 1, 2, \dots$$

Computing the r_j moments, is not trivial since $R(\mu)$ is evaluated using the complicated Fresnel relations that include absorption, Isard [7], Harpole [6]. The boundary condition is,

$$\begin{aligned} E &= \left(\frac{1 + 3r_2}{1 - 2r_1} \right) \left(\frac{2}{3\kappa} \right) (\hat{\mathbf{n}} \cdot \nabla E) \\ &= 4\pi n^2 \mathcal{B}_\nu(T_a)/v_g, \end{aligned} \quad (6)$$

where n and v_g are properties of material b . By setting r_j to zero, letting $n = 1$ and replacing v_g with c , we obtain the familiar Milne condition.²

Interface condition

²Note that $\hat{\mathbf{n}}$ is the *inward* normal.

Now assume that equations are to be solved in both materials, a and b , i.e., the interface of Fig.(2) is inside the computational domain. As in the previous section, in material b , the intensity emanating from the interface is a sum of two parts. One part is the fraction of intensity in material b , directed toward the interface, that is reflected back. Another part is the intensity transmitted from material a .

Equation (6) relates the radiation energy E on the surface of the material, and its normal derivative, to a term proportional to the external radiation energy. At steady-state, the derivative vanishes and $E = 4\pi n^2 \mathcal{B}_\nu(T_a)/v_g$. Equation (6) was derived assuming the external medium is a black body at temperature T_a , the external refractive index equals one, and externally, radiation propagates at speed c . Thus, the steady-state radiation energy density is *discontinuous* at the air-silica interface. The silica energy differs from the external value by the factor $n^2 c/v_g$. The discontinuity complicates obtaining a numerical solution if: (1) It is obtained by point-centered scheme that solves for surface values, and (2) The numerical domain extends over both media.

To avoid computing a discontinuous field, we introduce a new dependent variable,

$$\xi \doteq (1/n^2) \int_{4\pi} d\omega I. \quad (7)$$

The field ξ has the same units as I . If the n^2 factor is neglected, ξ is identical to the *scalar flux* of neutron transport theory. Using ξ as the dependent variable brings another benefit. In refractive media, I/n^2 , not I , is conserved along field lines [10].

The derivation of the equation for ξ is similar to the one for E . After some algebra, we find

$$\frac{1}{v_g} \partial_t \xi - \nabla \cdot \frac{1}{3\kappa} \nabla \xi = \kappa [4\pi \mathcal{B}_\nu(T) - \xi]. \quad (8)$$

Boundary and interface conditions for ξ are

obtained using the two-term expansion for the intensity in terms of ξ ,

$$I/n^2 = (1/4\pi) [\xi - (1/\kappa) \mathbf{\Omega} \cdot \nabla \xi]. \quad (9)$$

Equation (9) and a derivation similar to the one that led to Eq.(6) yields the boundary condition at a diffuse external source,

$$\xi - \left(\frac{1 + 3r_2}{1 - 2r_1} \right) \left(\frac{2}{3\kappa} \right) (\hat{\mathbf{n}} \cdot \nabla \xi) = 4\pi \mathcal{B}_\nu(T_a), \quad (10)$$

where, as before, $\hat{\mathbf{n}}$ is the inward normal. The derivation assumes $n = 1$ in the external medium. When the gradient vanishes, Eq.(10) implies that the surface value ξ equals $4\pi \mathcal{B}_\nu(T_a)$, i.e., ξ is continuous.

The derivation of the internal material interface condition is similar to that for the boundary condition. We first focus attention on the relation just inside material b , see Fig. 2. In the following, quantities in material b are not subscripted by b , while those in a carry the subscript.

The difference between the interface and boundary condition is that the transmitted radiation $I_t(\mathbf{\Omega})$ stems from non-diffuse radiation in material a that streamed along a direction $\mathbf{\Omega}_{a,i}$, see Fig. 2. Also, in material a , the intensity is given by Eq. (9), with $\mathbf{\Omega}$ replaced by $\mathbf{\Omega}_{a,i}$. The directions $\mathbf{\Omega}$ and $\mathbf{\Omega}_{a,i}$ are related via the Fresnel equation. For absorptive media, the relation is [6],

$$F(\beta_a, \theta_a) n_a \sin \theta_a = F(\beta, \theta) n \sin \theta,$$

where $\beta = (k/n)^2$ and analogously for β_a . The symbol k is the absorption index³. The angles θ and θ_a are those between $\mathbf{\Omega}$ and $\mathbf{\Omega}_{a,i}$ and the interface normal, resp. The square of F ,

$$[F(\beta, \theta)]^2 = 1 - \beta + \sqrt{(1 - \beta)^2 + 4\beta / \cos^2 \theta},$$

and analogously for $F(\beta_a, \theta_a)$. It is easy to show that for small angles, θ or θ_a , $F \approx \sqrt{2}$. Hence, for

³The opacity $\kappa = 4\pi k/\lambda$, with λ the vacuum wavelength.

near normal incidence, the absorptive Fresnel law reduces to the simpler non-absorptive variant,

$$n_a \sin \theta_a = n \sin \theta. \quad (11)$$

In the following, we will use Eq. (11) to derive the interface condition since one can easily express one angle or its differential in terms of the other.⁴

The major difficulty in deriving the condition is due to integrating the transmitted radiation over the hemisphere in material b . The transmitted radiation stems from a non-diffuse intensity in material a , i.e., it has the same form as Eq.(9), but with terms subscripted with a . After some algebra, we obtain the following expression for material b ,

$$\begin{aligned} & \xi - \left(\frac{1 + 3r_2}{1 - 2r_1} \right) \left(\frac{2}{3\kappa} \right) (\hat{\mathbf{n}} \cdot \nabla \xi) = \\ & \xi_a - \left(\frac{1}{1 - 2r_1} \right) \left(\frac{2}{\kappa_a} \right) (\hat{\mathbf{n}} \cdot \nabla \xi_a) J, \end{aligned} \quad (12)$$

where

$$J = \int_0^1 d\mu \mu [1 - R(\mu)] \sqrt{1 - \frac{n^2}{n_a^2} (1 - \mu^2)},$$

and, as before, R is the reflectivity. If $n > n_a$, there is no danger with negative values under the root since $R \rightarrow 1$ as the term in the root turns negative. Equation (12) reduces to a relation between the two gradients since ξ is continuous, i.e., $\xi = \xi_a$.

Equation (12) arises after integrating over the hemisphere in material b . When we perform an analogous hemispherical integration of the intensities in material a , and combine the result with Eq.(12), we obtain the desired condition,

$$\begin{aligned} & (1/\kappa) \hat{\mathbf{n}} \cdot \nabla \xi (1 + 3r_2 + 3J_a) = \\ & (1/\kappa_a) \hat{\mathbf{n}} \cdot \nabla \xi_a (1 + 3r_{2,a} + 3J), \end{aligned} \quad (13)$$

where,

$$J_a = \int_0^1 d\mu_a \mu_a [1 - R(\mu_a)] \sqrt{1 - \frac{n_a^2}{n^2} (1 - \mu_a^2)}.$$

⁴We can also express one angle in terms of the other using the general Fresnel relation, but the equation is messy.

The integrals J and J_a differ in that J integrates over the material b hemisphere while J_a integrates over material a , and similarly for the moments r_2 and $r_{2,a}$.

If materials a and b have the same index of refraction, the Fresnel equation is a tautology and Eq.(13) reduces to

$$(1/\kappa) \hat{\mathbf{n}} \cdot \nabla \xi = (1/\kappa_a) \hat{\mathbf{n}} \cdot \nabla \xi_a$$

The relation is consistent with Eq.(8); it states that fluxes of ξ are continuous.

Results, Cooling two materials

The equations for E are implemented in ALE3D. In August 2010, although RADMGDIFF allowed multiple materials and the material-dependent opacities could vary with temperature, the interface condition Eq.(13) had not been incorporated. Hence, for multiple material simulations, RADMGDIFF could only be used as a conventional radiation multigroup diffusion solver ($n = 1, v_g = c$). A number of simulations were made to test the code. Here we present a comparison with Lasnex.

Consider a 1D slab of SiO_2 , 1 cm thick, initially at $T = 2500$ °K. The slab is bounded by air on both sides, where $T_a = 298.15$. For $0 < Z < 0.5$, the heat capacity $C = 2.201 \cdot 10^7$ erg/cc °K, the conductivity $k_m = 2.201 \cdot 10^5$ erg/cm s °K, and the opacity κ is as shown in Fig.1. For $0.5 < Z < 1$, we use a tenfold smaller C and k_m , and have κ proportional to T so it increases tenfold from the Fig.1 value at $T = 100$ to 5000.

The comparison ALE3D with Lasnex appears in Table I, where we display results after 1 sec. The first six rows represent the maximum, left, and right matter and radiation temperatures. The last three are the final matter and radiation energies and the accumulated energy coupled (J/radian), which also equals the energy that exited through the boundary. The magnitude of coupled energy

illustrates the efficiency of radiation as a means of energy transport. The final radiation energies are 10^{10} less than what the field absorbed from the matter and radiated out.

Table I: Slab cooling problem; ALE3D, LASNEX comparison; 16 groups; $t = 1$ s; maximum, left-, right-side temperatures (°K); matter, radiation, coupled energies (J/radian)

	LAS	A3D($n=1$)
$\max(T_m)$	2477.3	2478.5
$\max(T_r)$	1555.6	1549.4
$T_{m,l}$	2428.8	2404.2
$T_{r,l}$	1424.5	1411.3
$T_{m,r}$	1687.0	1578.7
$T_{r,r}$	1328.9	1286.2
$E_m \cdot 10^{-3}$	1.4704	1.4675
$E_r \cdot 10^{-15}$	1.9469	1.9194
$E_c \cdot 10^{-5}$	4.2706	4.5668

Results, TopHat

To illustrate, RADMGDIFF's 3D performance, we consider the "Crooked Pipe" aka "TopHat" test problem of Graziani [4] using the specifications of Gentile [5]. The numerical domain consists of a quadrant of a 7 cm long cylinder, with radius = 2. The cylinder consists of two materials; one thick with opacity 2000 cm^{-1} and one thin with $\kappa = 0.2$. The domain is similar to a thick walled pipe with the inside (thin) material largely contained inside a 0.5 cm radius. However, inside the pipe, for $2.5 < Z < 4.5$, the thin domain expands to a 1.5 cm radius. Centered in the expanded thin cylinder is another cylinder, effectively an obstruction, consisting of the same thick material as the pipe walls. The obstruction extends over $3 < Z < 4$ and has a 1 cm radius. The computational mesh over just the thick region is displayed in Fig. 3. However, the numerical extends over both thick and thin materials.

DB: test10_001.00000
 Cycle: 0 Time: 0
 Mesh
 Var: mesh_3d

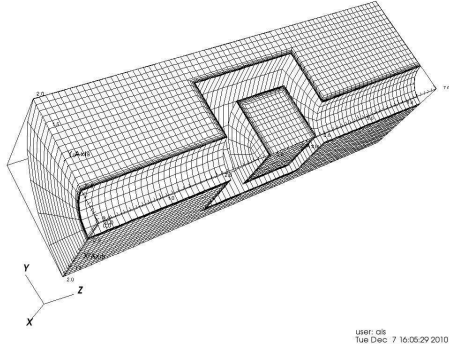


Figure 3: TopHat test problem, 3D mesh over thick material.

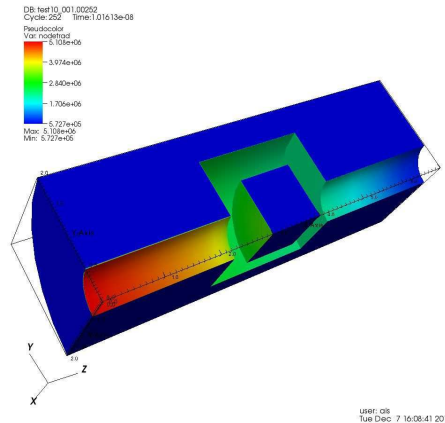


Figure 4: TopHat test problem, radiation temperature T_r in thick material, $t = 10$ ns.

The initial temperature is $T = 50$ eV in both materials. At $t = 0$, at one end of the thin material, we impose a Milne condition with a source temperature $T_s = 500$ eV. Symmetry is imposed on the azimuthal sides $\phi = 0, \pi/2$ and vacuum conditions are imposed on all other boundaries. We solve in gray mode, i.e., with just one group. The simulation is run to $t = 10$ ns.

Figure 4 displays the radiation temperature T_r over the thick domain. Note that because of the high opacity, radiation has raised T_r primarily only on the surfaces separating thick and thin materials; very little radiation has propagated inside.

Figure 5 displays T_r over the thin domain. Radiation has propagated over most of the domain.

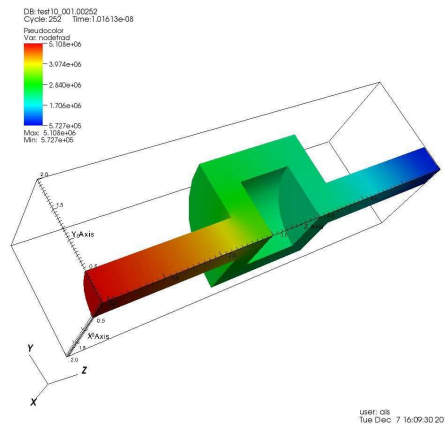


Figure 5: TopHat test problem, radiation temperature T_r in thick material, $t = 10$ ns.

Acknowledgments:

We thank Dr. J. Castor (LLNL) for drawing attention to issues related to maintaining LTE across a material interface. We thank Dr. T. Brunner (LLNL) for supplying the mesh for the TopHat problem.

Prepared for Proceedings of the NECDC 2010

References

- [1] M. Born and E. Wolf, *Principles of Optics*, Pergammon Press, Oxford (1975)
- [2] E. U. Condon, "Radiative transport in hot glass," *J. Quant. Spectrosc. Radiat. Transfer*, **28**, 369-385 (1968)
- [3] R. Gardon, "A review of radiant heat transfer in glass," *J. Amer. Ceramic Soc.*, **44**, 7, 305-312 (1961)
- [4] F. R. Graziani and J. LeBlanc, "The crooked pipe test problem," Technical Report UCR-MI-143393, Lawrence Livermore National Laboratory (2000)
- [5] N. A. Gentile, "Implicit Monte Carlo diffusion—An acceleration method for Monte Carlo time-dependent radiative transfer simulations," *J. Comp. Phys.*, **172** (2), 543-571 (2001)
- [6] G. M. Harpole, "Radiative absorption by evaporating droplets," *Int. J. Heat Mass Transfer*, **23**, 17-26 (1980)
- [7] J. O. Isard, "Surface reflectivity of strongly absorbing media and calculation of the infrared emissivity of glasses," *Infrared Phys.*, **20**, 249-256 (1980)
- [8] R. Kitamura, L. Pilon and M. Jonasz, "Optical constants of silica glass from extreme ultraviolet to far infrared at near room temperature," *Applied Optics*, **46**, 33, 8118-8133 (2007)
- [9] E. W. Larsen, G. Thömmes, A. Klar, M. Seaid and T. Götz, "Simplified P_N Approximations to the Equations of Radiative Heat Transfer and Applications," *J. Comp. Phys.*, **183**, 652-675 (2002)
- [10] G. C. Pomraning, *The Equations of Radiation Hydrodynamics*, Dover Pub. Inc., Mineola, New York (2005)
- [11] A. I. Shestakov, R. M. Vignes and J. S. Stölken, "Derivation and solution of multifrequency radiation diffusion equations for homogeneous refractive lossy media," Lawrence Livermore National Laboratory, LLNL-JRNL-422310-REV1, to appear in *J. Comp. Phys.*, (2010)